

## Evaluation of the Effects of Absorption Enhancers on Caco-2 Cell Monolayers by Using a Pore Permeation Model Involving Two Different Sizes

Toshinobu Seki,\* Airi Hamada, Yuya Egawa, Tsutomu Yamaki, Masaki Uchida, Hideshi Natsume, Soichiro Kimura, and Hideo Ueda

*Faculty of Pharmaceutical Sciences, Josai University; 1-1 Keyakidai, Sakado, Saitama 350-0295, Japan.*

Received June 13, 2013; accepted August 11, 2013

We applied a parallel pore permeation model based on the Renkin molecular sieving function by using two different-sized pathways to analyze the permeation-enhancing effects of poly-L-arginine (PLA) or a mixed system of spermine (SPM) and sodium taurocholate (STC). Four paracellular markers were simultaneously applied to Caco-2 cell monolayers, and a set of apparent permeability coefficient ( $P$ ) values was used to obtain membrane parameters. For PLA treatment, the pore occupancy/length ratio ( $\varepsilon/L$ ) of the large pathways increased while the pore radius ( $R$ ) did not, suggesting that the number of large pathways for the relatively large hydrophilic molecules in the monolayers could be increased by the addition of PLA. In contrast, application of the mixed system comprising SPM and STC significantly increased not only the  $R$  of the large pathways but also  $\varepsilon/L$  of the small pathways. Such changes in membrane parameters could be related to the enhancing mechanism of these compounds. The simulation curves for molecular weight (MW)- $P$  calculated from the membrane parameters could be used to predict the  $P$  of drugs with different MWs.

**Key words** permeation enhancer; Caco-2 cell; poly-L-arginine; spermine; sodium taurocholate; Renkin function

Several types of absorption enhancers such as surfactants, bile salts, fatty acids, and cationic compounds have been evaluated for their ability to increase the permeation of water-soluble drugs, including peptide and protein drugs with high molecular weights (MW) through mucous membranes.<sup>1,2)</sup> The choice of the enhancer and method of administration should be carefully made on the basis of knowledge about the enhancing mechanism(s) and physicochemical properties of the active drugs to be delivered.

The cationic polymer poly-L-arginine (PLA) improves the absorption of peptide and protein drugs through mucosal membranes while causing negligible damage to these membranes.<sup>3–5)</sup> PLA can open the tight junctions (TJs) between epithelial cells and increase the intercellular (paracellular) permeation of water-soluble drugs. Similar enhancing effects have been observed for sperminated polymers used to enhance the pulmonary and nasal absorption of water-soluble drugs.<sup>6,7)</sup> Spermine (SPM) is a cationic component found in cells and has been recognized as a permeation enhancer; SPM used with sodium taurocholate (STC) markedly enhanced the oral absorption of a drug categorized as Class IV, poorly absorbed, by the Biopharmaceutics Classification System.<sup>8)</sup> The combined use of SPM and STC not only opens TJs but also increases transcellular permeation of drugs. Such critical differences in the mechanisms of action should be considered for appropriate selection of the optimal enhancer.

In our previous studies, the Renkin molecular sieving function, which characterizes the porous permeation pathways in terms of the equivalent cylindrical pore radius ( $R$ ) and pore occupancy/length ratio ( $\varepsilon/L$ ), was used to evaluate the paracellular permeation pathways of epithelial membranes.<sup>9,10)</sup> When cationized polymers were applied as absorption enhancers for peptide drugs across epithelial membranes, the apparent

permeability coefficients ( $P$ ) of the paracellular markers used as model compounds for the peptide drugs enhanced. The  $P$  values were fitted to the Renkin function to evaluate the change in the  $\varepsilon/L$  and  $R$  of the membranes. The results of the fit indicated an increase only for the  $\varepsilon/L$ , not for the  $R$ , suggesting that the number of pathways for hydrophilic molecules in the membranes increased upon the addition of the enhancers. Although there are at least two different-sized permeation pathways in epithelial membranes, the changes we observed in the membrane parameters could be accounted for by only the relatively large pathways. Little information could be obtained for the smaller pathways. In order to examine both pathways, a parallel pore permeation model involving two different-sized pathways must be employed.<sup>11)</sup> The small pathways might have particularly closed TJs, but these might be made apparently more permeable by using enhancers that generate transcellular pathways for small paracellular markers. Therefore, a methodology using both the Renkin function and the parallel pore permeation model with two different-sized pathways could be used to evaluate the mode of action for different penetration enhancers.

In the present report, the Renkin function was applied to determine the mode of action for PLA and for a mixed system of SPM and STC on the hydrophilic pathways including not only large but also small pathways in Caco-2 cell monolayers. Four paracellular markers having different diffusivity ( $D$ ) were simultaneously applied to the monolayers and a set of  $P$  values was used to obtain the  $\varepsilon/L$  and  $R$  values of the small and large pathways for each monolayer sample. Nonmetabolic oligosaccharides and sugar alcohols were used as markers.<sup>12)</sup> Thus, a change in the  $\varepsilon/L$  and  $R$  values following the addition of the enhancers could be related to the enhancers' effects on the hydrophilic penetration pathways.

The authors declare no conflict of interest.

\* To whom correspondence should be addressed. e-mail: sekt1042@josai.ac.jp

## MATERIALS AND METHODS

**Materials** Xylitol (XT, MW: 152.2), *meso*-erythritol (ET, MW: 122.1), and inulin (IN, MW: 4268) were purchased from Wako Pure Chemical Industries, Ltd. (Osaka, Japan). Iso-maltose (IM, MW: 342.3) was obtained from Tokyo Chemical Industry (Tokyo, Japan). PLA (MW: 15000–70000) and fluorescein isothiocyanate (FITC)-dextran (FD4, MW: 4400) were purchased from Sigma-Aldrich Japan (Tokyo). SPM and STC were products of Wako Pure Chemical Industries, Ltd. All other chemicals were of reagent grade or HPLC grade and used as received.

**Cell Culture** Caco-2 cells were obtained from Riken Gene Bank (Ibaraki, Japan). The cells were maintained in Dulbecco's modified Eagle's medium (DMEM) containing 10% heat-inactivated fetal calf serum, 40  $\mu$ g/mL gentamicin, and 1% nonessential amino acids in a humidified atmosphere of 95% air and 5% CO<sub>2</sub> at 37°C. The cells were seeded ( $4.5 \times 10^5$  cells/cm<sup>2</sup>) on polycarbonate filter inserts (pore size: 0.4  $\mu$ m; area: 4.7 cm<sup>2</sup>; Transwell, Costar) and cultivated until transepithelial resistance (TER) increased over 500  $\Omega$ ·cm<sup>2</sup>. TER was measured using Millicell®-ERS (Millipore, MASS, U.S.A.).

**Permeation Experiments** An isotonic solution containing IN (20 mg/mL), IM (90 mM), ET (90 mM), and XT (90 mM) was mixed with the same volume of Hanks' balanced salt solution (HBSS), and the mixed solution was applied to the monolayers. The initial TER was then measured. HBSS was used as the basolateral side solution. In the enhancer-treating experiments, PLA (0.20%) or the combination of SPM (5.0 mM) and STC (10 mM) was added to the mixed solution. The receiver solution in the basolateral side of the layers was collected every 15 min for 120 min. Then, cell viability was checked using the 3-(4,5-dimethylthiazol-2-yl)-2,5-diphenyltetrazolium bromide (MTT) assay.<sup>13</sup> Cell viability after PLA and after the mixed-system treatment was 86.3% $\pm$ 6.3% and 94.5% $\pm$ 17.7%, respectively. Although cell viability after PLA treatment was lower than that after mixed-system treatment, there was no significant difference between either value and the control value (98.8% $\pm$ 15.0%).

A dual-pump HPLC system (LC10; Shimadzu, Kyoto, Japan) with a charged aerosol detector (CAD, ESA Biosciences, MA, U.S.A.) was used to determine the concentration of the paracellular markers. Tandem-connected Shodex SC-2G, SC1011, and SC1821 columns (SHOWA DENKO, Tokyo, Japan) were used for the separation of IM, XT, and ET at 80°C. For IN determination, a Shodex SB-803HQ column (SHOWA DENKO) was used separately at 60°C. A pump provided water at 0.5 mL/min as the mobile phase, which passed through the injector and columns. Another pump was used to

provide acetonitrile at 0.5 mL/min to increase the sensitivity of the CAD. The water from the column and acetonitrile were introduced into a mixer, and the outlet of the mixer was connected to the CAD. Solution samples (20  $\mu$ L) were injected two times for different column systems.

**Analysis Using the Renkin Function** The Renkin function (Eq. 1S or 1L) was used for characterization of the paracellular absorption pathways.<sup>9,11)</sup>

$$F\left(\frac{r_i}{R_s}\right) = \left(1 - \left(\frac{r_i}{R_s}\right)\right)^2 \times \left[1 - 2.104\left(\frac{r_i}{R_s}\right) + 2.09\left(\frac{r_i}{R_s}\right)^3 - 0.95\left(\frac{r_i}{R_s}\right)^5\right] \quad (1S)$$

$$F\left(\frac{r_i}{R_L}\right) = \left(1 - \left(\frac{r_i}{R_L}\right)\right)^2 \times \left[1 - 2.104\left(\frac{r_i}{R_L}\right) + 2.09\left(\frac{r_i}{R_L}\right)^3 - 0.95\left(\frac{r_i}{R_L}\right)^5\right] \quad (1L)$$

where  $R_s$  and  $R_L$  are pore radii of small and large pathways, respectively, and  $r_i$  is the molecular radius of penetrant  $i$ . Although the  $r_i$  values can be calculated from the diffusion coefficient of  $i$  ( $D_i$ ) as the Stokes–Einstein radius ( $r_{SE}$ ), for small molecules (MW: <272.5), the hydrodynamic radius ( $r_{HYD}$ ) can be calculated from the following equation (Eq. 2).<sup>14)</sup> The  $r_{SE}$  or  $r_{HYD}$  was used for the analysis as  $r_i$  value.

$$r_{HYD} = \left(0.92 + \frac{21.8}{MW}\right) \cdot r_{SE} \quad (2)$$

The apparent permeability coefficient ( $P_a$ ) of the paracellular markers was calculated according to the following equation (Eq. 3).

$$P_a = \frac{Flux_{ss}}{C_d} \quad (3)$$

where  $Flux_{ss}$  is the steady-state permeation rate of the marker, and  $C_d$  is the initial concentration in the applied solution. In the parallel pore permeation model involving two different-sized pathways,  $P_a$  was considered the sum of the permeability coefficient for small pathways ( $P_s$ ) and large pathways ( $P_L$ ) according to the following equation (Eq. 4).

$$P_a = P_s + P_L \quad (4)$$

The  $P$  values of both pathways are functions of the Renkin function, the pore occupancy of the pathways ( $\epsilon_s$  and  $\epsilon_L$ ), and the diffusivity and size of the permeating marker molecules (Table 1), as shown in Eqs. 5S and 5L.

Table 1. Diffusion Parameters of the Paracellular Markers and Permeability Coefficient of the Markers in Caco-2 Cell Monolayers

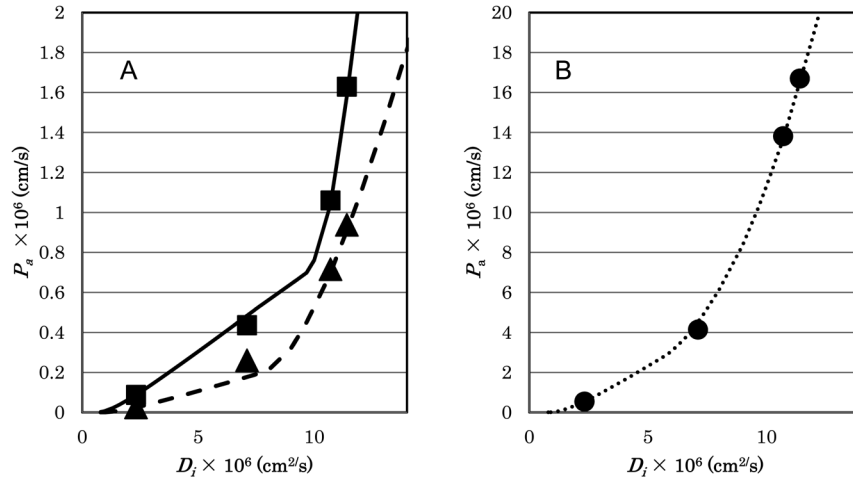
	MW	$r_i$ (nm)	$D$ (cm <sup>2</sup> /s)	Permeability coefficient, $P_a$ (cm/s) <sup>c)</sup>		
				Control	PLA	SPM+STC
IN	4268	1.41 <sup>a)</sup>	$2.32 \times 10^{-6}$	$3.21 \pm 0.51 \times 10^{-8}$	$3.99 \pm 2.33 \times 10^{-7**}$	$6.93 \pm 1.51 \times 10^{-8*}$
IM	342.3	0.459 <sup>a)</sup>	$7.11 \times 10^{-6}$	$3.29 \pm 1.15 \times 10^{-7}$	$2.61 \pm 1.23 \times 10^{-6**}$	$3.72 \pm 0.97 \times 10^{-7}$
XT	152.2	0.334 <sup>b)</sup>	$1.07 \times 10^{-5}$	$8.23 \pm 2.43 \times 10^{-7}$	$9.81 \pm 3.91 \times 10^{-6**}$	$8.14 \pm 2.60 \times 10^{-7}$
ET	122.1	0.320 <sup>b)</sup>	$1.14 \times 10^{-5}$	$1.07 \pm 0.27 \times 10^{-6}$	$1.19 \pm 0.44 \times 10^{-5**}$	$1.39 \pm 0.50 \times 10^{-6}$

a),  $r_{SE}$ ; b),  $r_{HYD}$ ; c, mean  $\pm$  S.D.; \* $p$  < 0.05 in Dunnett's test; \*\* $p$  < 0.01 in Dunnett's test.

Table 2. Membrane Parameters of Caco-2 Cell Monolayers in the Parallel Pore Permeation Model

	Control		PLA		SPM+STC	
	Large	Small	Large	Small	Large	Small
$r_p$ (nm)	$6.27 \pm 0.46$	$0.448 \pm 0.074$	$6.33 \pm 0.58$	$0.555 \pm 0.034$	$8.00^* \pm 0.81$	$0.354^* \pm 0.005$
$\varepsilon/L$ ( $\text{cm}^{-1}$ )	$0.0417 \pm 0.0063$	$12.5 \pm 8.3$	$0.527^* \pm 0.340$	$28.5 \pm 9.4$	$0.0699 \pm 0.0185$	$82.6^{**} \pm 7.0$

Mean  $\pm$  S.D.; \* $p < 0.05$  in Dunnett's test; \*\* $p < 0.01$  in Dunnett's test.

Fig. 1. Curve Fits for the  $D_i$ - $P_a$  Relationship in the Parallel Pore Permeation Model Based on the Renkin Function

A:  $\blacktriangle$ , control;  $\blacksquare$ , mixed system comprising SPM (5.0 mM) and STC (10 mM). B:  $\bullet$ , PLA (0.20%).

$$P_{S,i} = (\varepsilon_S / L) \cdot D_i \cdot F\left(\frac{r_i}{R_S}\right) \quad (5S)$$

$$P_{L,i} = (\varepsilon_L / L) \cdot D_i \cdot F\left(\frac{r_i}{R_L}\right) \quad (5L)$$

The  $P_a$  values of the four markers were used to obtain four different unknown membrane parameters  $\varepsilon_S/L$ ,  $\varepsilon_L/L$ ,  $R_S$ , and  $R_L$  for each cell monolayer. The obtained parameters were used to draw the simulation curve of  $P_a$ - $D$ . The simulation curves of  $P_a$ -MW were also constructed using these parameters obtained along with the following relationship between MW and  $D$ .<sup>15)</sup>

$$\log D = -0.4145 \cdot \log MW - 4.111 \quad (6)$$

**FD4 Permeation Study** Separately cultured Caco-2 cell monolayers were used for FD4 permeation experiments to validate the analysis. FD4 solution (50 mg/mL, in HBSS) in the presence or absence of enhancers was applied to the apical side of the monolayers. HBSS was used as the basolateral side solution, and this was changed every 15 min for 120 min. The FD4 concentration was determined using a spectrofluorometer (RF-5300, Shimadzu) at an excitation wavelength of 495 nm and an emission wavelength of 519 nm.

## RESULTS AND DISCUSSION

The  $P_a$  values for the markers permeating the Caco-2 cell monolayers are summarized in Table 1. The permeability-enhancing effect of PLA was stronger than that of the mixed system comprising SPM and STC. While permeation of all markers significantly increased upon addition of PLA, the effect of the mixed system was significant only for IN. A set

of  $P_a$  values for the markers was used to obtain the four membrane parameters. The parameters giving a good curve fit are shown in Table 2; representative curve fits are shown in Fig. 1. For PLA treatment, the  $\varepsilon_L/L$  of the monolayers increased while the  $R_L$  did not, suggesting that the number of large pathways for relatively large hydrophilic molecules in the monolayers could be increased by the addition of PLA. Similar results for PLA were observed in an *in vivo* nasal absorption experiment in rats.<sup>16)</sup> Although no significant differences were observed for the small pathways, both  $\varepsilon_S/L$  and  $R_S$  values were higher. This result suggests that some aspect of the TJs might have opened following the addition of PLA, increasing the number of large pathways. The increase in  $\varepsilon_S/L$  and  $R_S$  might be related to PLA's unexpected action of TJ opening. In contrast to PLA, the addition of the mixed system comprising SPM and STC significantly increased the  $R_L$  value, and the high value of  $\varepsilon_L/L$  was explained by a radius-dependent increase in the area pathway. These results suggest that while the number of large pathways cannot be changed by the mixed system, the size of each pathway increases. The parameters of the small pathways,  $\varepsilon_S/L$  and  $R_S$ , were also changed by the addition of the mixed system. The  $R_S$  value is related to the sieving property of membranes, and a great dependency of molecular size on the permeability implies a confined pathway. The low values of  $R_S$  observed cannot be due to a change in the small pathways of the TJs. Because the mixed system comprising SPM and STC acts on paracellular pathways as well as on transcellular pathways, small hydrophilic compounds such as ET could permeate cell membranes following the addition of the mixed system. The sieving property of these newly generated pathways might influence the  $R_S$  values. The high  $\varepsilon_S/L$  value suggests a high occupancy of these new pathways within the small pathways as the sum of paracellular and tran-

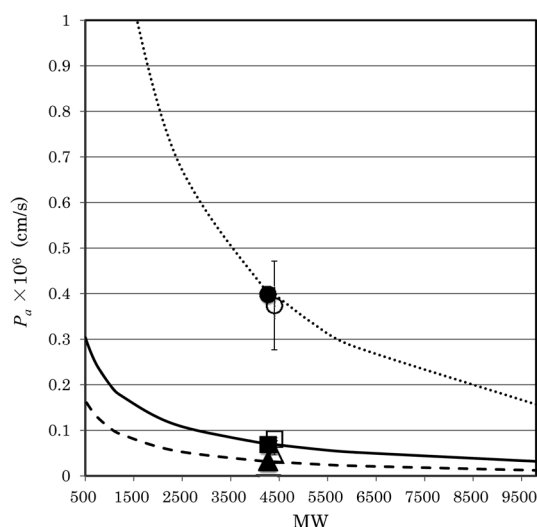


Fig. 2. Simulation Curves for the MW- $P_a$  Relationship Calculated Using the Four Membrane Parameters Obtained, MW- $D$  Relationship, and  $P_a$  Values of IN and FD4

Simulation curves: —, control; —, mixed system comprising SPM (5.0mm) and STC (10mm); ---, PLA (0.20%). Curves are drawn using the Renkin functions, Eq. 6, and the parameters in Table 2.  $P_a$ : IN (used to obtain the curves), control ( $\blacktriangle$ ), mixed system comprising SPM and STC ( $\blacksquare$ ), PLA ( $\bullet$ ); FD4 (not used to obtain the curves, mean  $\pm$  S.D.), control ( $\triangle$ ), mixed system comprising SPM and STC ( $\square$ ), PLA ( $\circ$ ).

scellular pathways for small molecules.

In the mechanism of the penetration enhancement for PLA, the TJ proteins occludin, ZO-1, claudin-4, and tricellulin can be internalized in the cell by clathrin-mediated endocytosis.<sup>13)</sup> This internalization should be directly related with the increasing number of large pathways. When a clathrin-mediated endocytosis inhibitor was used with PLA in Caco-2 cell experiments, the enhancing effect for FD4 was suppressed while the effect on ET permeation remained. If there are two steps involved in the permeation-enhancing mechanism of PLA, an initial structural change in TJs and latter internalization of TJ proteins, then the two steps together may induce a large pathway increase, while the initial structural change may affect permeation only *via* the small pathways.

The mixed system comprising SPM and STC can affect both intercellular and paracellular pathways.<sup>8)</sup> Several mechanisms to increase paracellular permeability have been suggested, and one of the possible mechanisms pertaining to the mixed system could be the opening of TJs by myosin light-chain kinase activation related to an inositol-triphosphate-dependent  $\text{Ca}^{2+}$  release from the endoplasmic reticulum.<sup>17)</sup> SPM can increase the intracellular  $\text{Ca}^{2+}$  concentration *via* the inositol-triphosphate pathway in rat intestine.<sup>18)</sup> A TJ opening with an increased  $R_L$  value might induce increased permeation of bigger molecules such as IN. The enhanced transcellular permeation might be related to the increase in membrane fluidity by the mixed system comprising SPM and STC.<sup>19)</sup> Although the permeability-enhancing effects of the mixed system for the paracellular markers used were not as strong as for those of PLA, this does not imply a lower potential of the mixed system. The mixed system can be applied as a possible enhancer for various drugs that can permeate cell membranes.

The membrane parameters and the relationship between MW and  $D$  (Eq. 6) were used to calculate simulation curves between MW and  $P_a$ . The resulting curves are shown in Fig.

2. These curves predict the  $P_a$  of drugs having different MW and the effects enhancers might have on them. To test the validity of these predictions, a permeation study for FD4, a widely used paracellular marker, was conducted separately. The resulting  $P_a$  values for FD4 are plotted in Fig. 2 and support our analysis. However, FD4 is not the ideal test marker because the MW of FD4 is similar to that of IN, FD4 may have specific interactions with the cell surface, and FD4 may contaminate free fluorescein. Therefore, additional marker compounds that are nonmetabolic paracellular markers and model peptides with different MWs should be tested as the next step.

In conclusion, we applied the parallel pore permeation model based on the Renkin molecular sieving function by using two different-sized pathways for the analysis of the permeation-enhancing effects of PLA and the mixed system comprising SPM and STC. The change in the four membrane parameters following the addition of the enhancers was related to their mechanisms for enhancing permeation. The simulation curves for MW- $P_a$  calculated from the membrane parameters could be used to predict the  $P_a$  values of drugs having different MWs.

## REFERENCES

- 1) Renukuntla J, Vadlapudi AD, Patel A, Boddu SHS, Mitra AK. Approaches for enhancing oral bioavailability of peptides and proteins. *Int. J. Pharm.*, **447**, 75–93 (2013).
- 2) Williams AC, Barry BW. Penetration enhancers. *Adv. Drug Deliv. Rev.*, **56**, 603–618 (2004).
- 3) Miyamoto M, Natsume H, Satoh I, Ohtake K, Yamaguchi M, Kobayashi D, Sugibayashi K, Morimoto Y. Effect of poly-L-arginine on the nasal absorption of FITC-dextran of different molecular weights and recombinant human granulocyte colony-stimulating factor (rhG-CSF) in rats. *Int. J. Pharm.*, **226**, 127–138 (2001).
- 4) Ohtake K, Maeno T, Ueda H, Ogihara M, Natsume H, Morimoto Y. Poly-L-arginine enhances paracellular permeability *via* serine/threonine phosphorylation of ZO-1 and tyrosine dephosphorylation of occludin in rabbit nasal epithelium. *Pharm. Res.*, **20**, 1838–1845 (2003).
- 5) Yamaki T, Uchida M, Kawahara Y, Shimazaki Y, Ohtake K, Kimura M, Uchida H, Kobayashi J, Ogihara M, Morimoto Y, Natsume H. Effect of poly-L-arginine on intestinal absorption of hydrophilic macromolecules in rats. *Biol. Pharm. Bull.*, **36**, 496–500 (2013).
- 6) Seki T, Kanbayashi H, Nagao T, Chono S, Tomita M, Hayashi M, Tabata Y, Morimoto K. Effect of aminated gelatin on the nasal absorption of insulin in rats. *Biol. Pharm. Bull.*, **28**, 510–514 (2005).
- 7) Seki T, Fukushi N, Chono S, Morimoto K. Effects of sperminated polymers on the pulmonary absorption of insulin. *J. Control. Release*, **125**, 246–251 (2008).
- 8) Mukaizawa F, Taniguchi K, Miyake M, Ogawara K, Odomi M, Higaki K, Kimura T. Novel oral absorption system containing polyamines and bile salts enhances drug transport *via* both transcellular and paracellular pathways across Caco-2 cell monolayers. *Int. J. Pharm.*, **367**, 103–108 (2009).
- 9) Seki T, Kanbayashi H, Nagao T, Chono S, Tabata Y, Morimoto K. Effect of cationized gelatins on the paracellular transport of drugs through Caco-2 cell monolayers. *J. Pharm. Sci.*, **95**, 1393–1401 (2006).
- 10) Seki T, Kanbayashi H, Chono S, Tabata Y, Morimoto K. Effects of a sperminated gelatin on the nasal absorption of insulin. *Int. J. Pharm.*, **338**, 213–218 (2007).
- 11) Seki T, Harada S, Hosoya O, Morimoto K, Juni K. Evaluation of the establishment of a tight junction in Caco-2 cell monolayers using a

- pore permeation model involving two different sizes. *Biol. Pharm. Bull.*, **31**, 163–166 (2008).
- 12) Seki T, Kiuchi T, Seto H, Kimura S, Egawa Y, Ueda H, Morimoto Y. Analysis of the rat skin permeation of hydrophilic compounds using the Renkin function. *Biol. Pharm. Bull.*, **33**, 1915–1918 (2010).
- 13) Yamaki T, Ohtake K, Ichikawa K, Uchida M, Uchida H, Ohshima S, Juni K, Kobayashi J, Morimoto Y, Natsume H. Poly-L-arginine-induced internalization of tight junction proteins increases the paracellular permeability of the Caco-2 cell monolayer to hydrophilic macromolecules. *Biol. Pharm. Bull.*, **36**, 432–441 (2013).
- 14) Avdeef A. Leakiness and size exclusion of paracellular channels in cultured epithelial cell monolayers-interlaboratory comparison. *Pharm. Res.*, **27**, 480–489 (2010).
- 15) Hosoya O, Chono S, Saso Y, Juni K, Morimoto K, Seki T. Determination of diffusion coefficients of peptides and prediction of permeability through a porous membrane. *J. Pharm. Pharmacol.*, **56**, 1501–1507 (2004).
- 16) Seki T, Hosoya O, Natsume H, Sato I, Egawa Y, Nakagawa H, Juni K, Morimoto Y. Application of the Renkin function to characterize paracellular pathways in the nasal absorption of FITC-dextran in rats. *J. Drug Del. Sci. Tech.*, **19**, 331–335 (2009).
- 17) Lindmark T, Kimura Y, Artursson P. Absorption enhancement through intracellular regulation of tight junction permeability by medium chain fatty acids in Caco-2 cells. *J. Pharmacol. Exp. Ther.*, **284**, 362–369 (1998).
- 18) Cheng SX, Geibel JP, Hebert SC. Extracellular polyamines regulate fluid secretion in rat colonic crypts via the extracellular calcium-sensing receptor. *Gastroenterology*, **126**, 148–158 (2004).
- 19) Higaki K, Kato M, Hashida M, Sezaki H. Enhanced membrane permeability and microviscosity. *Pharm. Res.*, **5**, 309–312 (1988).